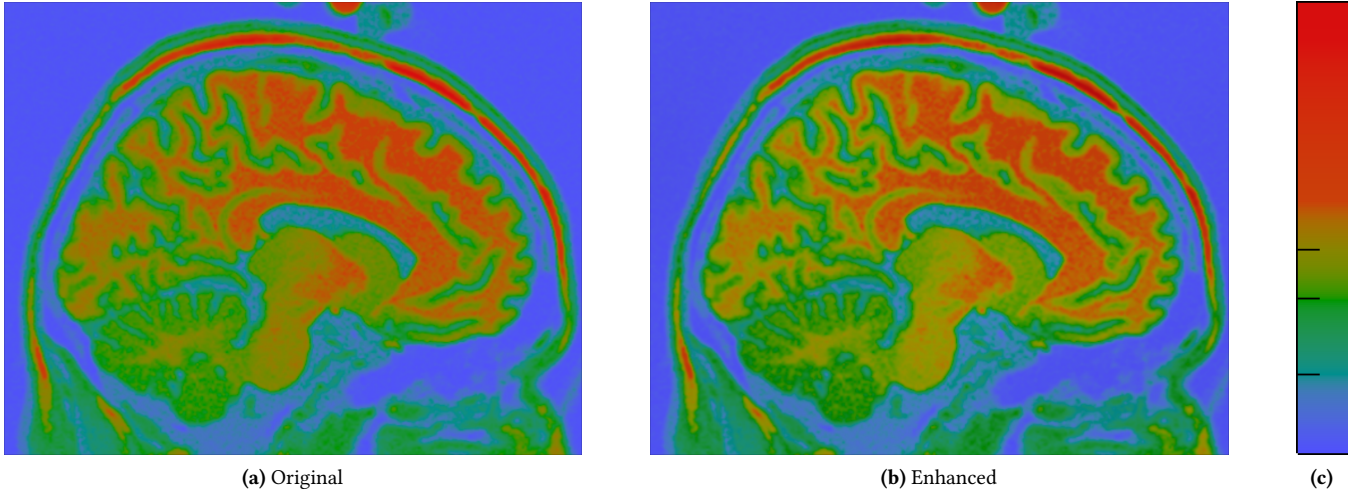


# Contrast Enhancement based on Viewing Distance

Anonymous Author(s)



**Figure 1.** Visualizations of the MRI brain dataset: (a) original, and (b) contrast enhanced by our method. The color map is shown in (c). Note that all figures in the paper are supposed to be shown on the screen with around 30 cm for the maximum extent and viewed at 80 cm away.

## Abstract

In this paper, we propose an image-space contrast enhancement method for color-encoded visualization. The contrast of an image is enhanced through a perceptually-guided approach that interfaces with the user with a single and intuitive parameter of the virtual viewing distance. To this end, we analyze a multiscale contrast model of the input image and test the visibility of bandpass images of all scales at a virtual viewing distance. By adapting weights of bandpass images with a threshold spatial vision model, this image-based method enhances contrast to compensate for contrast loss caused by viewing the image at a certain distance. Relevant features in the color image can be further emphasized by the user using overcompensation. The method is efficient and can be integrated into any visualization tool as it is a generic image-based post-processing technique. Using highly diverse datasets, we show the usefulness of perception compensation across a wide range of typical visualizations.

---

Permission to make digital or hard copies of part or all of this work for personal or classroom use is granted without fee provided that copies are not made or distributed for profit or commercial advantage and that copies bear this notice and the full citation on the first page. Copyrights for third-party components of this work must be honored. For all other uses, contact the owner/author(s).

VINCI'18, August 2018,

© 2018 Copyright held by the owner/author(s).

ACM ISBN 123-4567-24-567/08/06.

[https://doi.org/10.475/123\\_4](https://doi.org/10.475/123_4)

**Keywords** Contrast, visualization, perception

## ACM Reference Format:

Anonymous Author(s). 2018. Contrast Enhancement based on Viewing Distance. In *Proceedings of ACM VINCI conference (VINCI'18)*. ACM, New York, NY, USA, Article 4, 9 pages. [https://doi.org/10.475/123\\_4](https://doi.org/10.475/123_4)

## 1 Introduction

A faithful visual representation relies on both appropriate mapping of the data and the visual perception followed [18]. In this paper, we focus on the latter—visual perception in the context of visualizations, and specifically, color encoding of 2D images. In particular, we study the faithfulness of contrast representation caused by viewing distance. Our new method has the main effect of enhancing contrast depending on virtual viewing distance.

Color encoding is one of the main research topics in visualization [2, 24, 25, 28]. Here, we refer to color as a combination of achromatic and chromatic information. A large body of research focuses on rules and factors affecting the effectiveness of color coding. The perception of chromatic and achromatic information, together with the effect of spatial frequency and contrast has been studied [2, 25]. However, a controllable contrast enhancement method does not yet exist in the context of visualization to the best of our knowledge.

Our method is inspired by studies in human visual perception. The basis of our method is a threshold model of

spatial vision, i.e., a model that predicts the visibility of an object under different viewing conditions. The computation of contrast and contrast sensitivity functions (CSF) is the core of such a model. It is believed that the human visual system contains visual pathways in a band-pass fashion, and therefore, spatial vision can be appropriately modeled by multiscale models [20, 26, 27]. A multiscale contrast model is proposed by Peli [21] to address the contrast representation of a complex image. There, a bandpass image pyramid is built using either cosine-log filters of various scales or multiscale Gaussian filters. We adopt this contrast representation [21] and choose to use the cosine-log pyramid as it provides more accurate spatial frequencies. CSFs have been measured in physiological and psychophysical experiments [3, 16, 17, 27]. These measurements are successfully matched by computational models of CSFs. In particular, a computational model for multiscale CSFs is proposed to predict visible differences between two images by Daly [4]. This comprehensive model considers variables affecting the contrast sensitivity, including the illumination level, image size, stimuli orientation and viewing distance. Our contrast enhancement method combines the multiscale contrast model [21] with the computational CSF [4]; a virtual viewing distance is used as the single parameter to enhance contrast by adjusting band weights so that all band-pass images become visible.

Mullen [16] studies visual sensitivity for sinusoidal grating patterns for monochromatic luminance gratings and isoluminant chromatic gratings. The CSFs from experiments show that better visual sensitivity is achieved for chromatic channels for low spatial frequency stimuli, whereas the luminance channel provides better sensitivity for stimuli with higher spatial frequency. Therefore, we keep the chromatic channels for low spatial frequencies and use the viewing distance-adjusted achromatic image to provide more insights into higher spatial frequencies.

An example of the MRI brain dataset is shown as the original (Figure 1(a)), and enhanced by our method (Figure 8(b)) by our method. The enhanced result shows details inside the brain tissues that look washed away in the original visualization.

The contribution of our work is an efficient image-based technique that enhances contrast using a single parameter of virtual viewing distance. The method is inspired by the perception literature, and it goes beyond just compensation for contrast loss caused by viewing distance, but allows for flexible overcompensation to emphasize relevant features in the image.

One benefit of our approach is its generality: our method can be used for a wide range of visualization examples, ranging from volume visualization with transfer functions all the way to 2D geographic information visualization, as demonstrated in our examples. Another advantage is the simplicity of the image-based post-processing that does not interfere with previous steps in the visualization pipeline and can be

combined with any visualization system. Through our efficient computational model, the image enhancement works in interactive settings. Our method comes with easy and intuitive controllability with the virtual viewing distance as the only parameter.

## 2 Related Work

Utilizing color in computer-based visualization is an important research topic [28]. Luminance and spatial frequency aspects in visualizations with color mapping are in particular related to our work. Specifically, luminance is more effective for revealing high-spatial-frequency structures than chromatic channels [23, 25]. The spatial frequency of the data is considered an important factor in color map design [2]. Color maps and high-frequency sinusoid gratings are combined to design better perceptually uniform color maps that have good luminance contrast across the whole range [9].

Luminance also plays an important role to improve details in natural image processing. Tone mapping operators [5, 12, 22] are concerned with the compression of luminance range while preserving perceived contrast. Unlike our proposed method, these are image processing methods that target to reproduce the perceived image of high dynamic range input on low dynamic range devices, and cannot be tuned with a viewing distance.

Computational perception models exist, albeit outside of the field of visualization. Daly [4] predicts the visible differences between two images by devising a computational visual perception model. We make use of the CSF of [4] for threshold contrast computation in our method. The HDR visible difference predictor (HDR VDP) [13] is a perceptual model that compares a test high-dynamic-range image against a reference high-dynamic-range image and predicts the visibility, i.e., the visible differences between these images, and quality—the quality degradation with respect to the reference image. However, these models concern on generating image metric for natural-scened photos or synthesized images, while our method perceptually enhances potentially abstract visualizations.

In the context of visualization, perceptual aspects have been studied. Our paper is concerned with color perception in the context of its spatial embedding, and [7] is relevant to our work but with a different goal in mind. There, the visibility of features of different spatial frequencies at different viewing distances of a display wall is studied. A hybrid-image method that combines a near image containing high-frequency information with a far image that has low-frequency information is proposed to allow the user to perceive coarse features well at distance and acquire fine details when close to the display. We also analyze multiscale band-limited images, however, we utilize them to compensate for perception distortions and design perceptually oriented color transformation. Moreover, rather than a display-wall setting

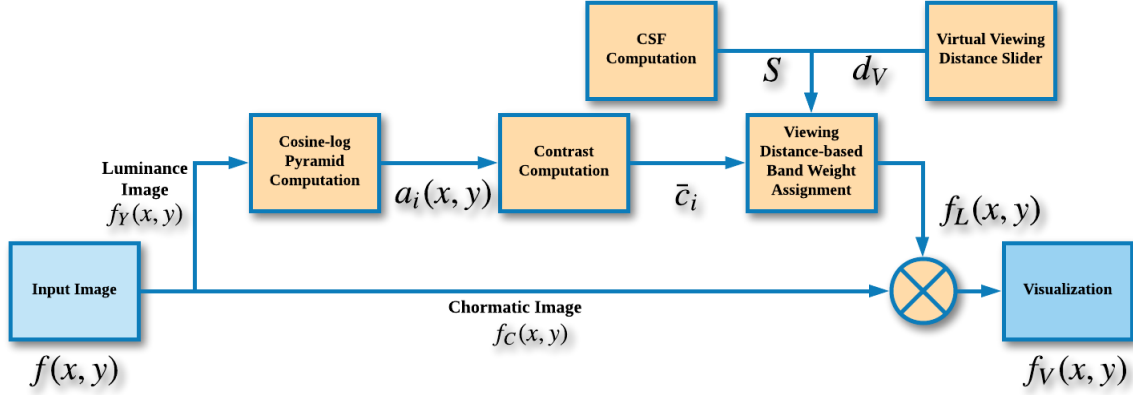


**Figure 2.** The workflow of our contrast enhancement method based on virtual viewing distance.

where the user moves back and forth [7], we focus on a typical working space setting where the user sits in front of a regular monitor at more or less a fixed distance.

In regard to compensation for perception effects, methods [14, 15] are proposed to compensate for the simultaneous contrast effect, which makes regions of the same color look different. The compensation is realized by setting these regions with different colors based on a customized color appearance model. Unlike their work, our method does not focus on the isolated simultaneous contrast effect but how viewing distance affects the contrast on different spatial scales. Furthermore, our method goes beyond compensation but also supports overcompensation, which is important for visualization.

Sufficient contrast is vital for gaining insights into the underlying data in a visualization. In fact, user studies [19] have shown that sharp boundaries created by binning continuous encodings help with the understanding of the data: participants with binned encoding outperform those with continuous encoding in terms of both the completion time and accuracy. Therefore, it is natural to enhance contrast for visualization images. Our method supports flexible interactive overcompensation through a slider, allowing for highlighting features of interest in a visualization. It is important to note that such overcompensation is not arbitrary but perceptually based in our method.

### 3 Methods

The input of our method is a color image  $f(x, y)$ . An image pyramid containing band-limited images  $a_i(x, y)$  is extracted using cosine-log filters from the luminance image  $f_Y(x, y)$  of  $f(x, y)$ . Then, average contrast  $\bar{c}_i$  of these band-limited images is calculated. Viewing distance-based band weight assignment is achieved by testing the  $\bar{c}_i$  against a CSF  $S$ , which is computed separately and independent of the dataset, for a given virtual viewing distance set by the user. The luminance difference image  $f_L(x, y)$  is then created by modulating the

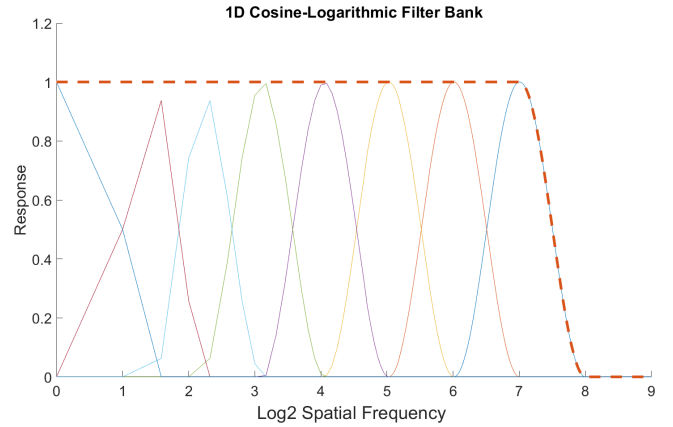


**Figure 3.** Filter bank of 1-octave-wide cosine-log 1D filters in the discrete spatial frequency domain. The dashed curve indicates the sum of all filters.

band weights with  $a_i(x, y)$ . The final visualization  $f_V(x, y)$  is created by combining the luminance difference image  $f_L(x, y)$  and the chromatic part  $f_C(x, y)$  of  $f(x, y)$ . The workflow of our method is illustrated in Figure 2. The remainder of this section explains each module in our pipeline in detail.

#### 3.1 Image Pyramid Generation

A multiscale model of spatial vision uses an image pyramid generated from the input image. An image  $f(x, y)$  can be described in the frequency domain with polar coordinates representation:

$$\begin{aligned} F(u, v) &= F(r, \theta) = L_0(r, \theta) + \sum_{i=1}^{l-1} A_i(r, \theta) + H_l(r, \theta), \\ &\approx L_0(r, \theta) + \sum_{i=1}^{l-1} A_i(r, \theta), \end{aligned} \quad (1)$$

$$r = \sqrt{(u^2 + v^2)}, \theta = \arctan\left(\frac{v}{u}\right),$$

where  $u$  and  $v$  are the horizontal and vertical spatial frequency coordinates in cycles/image [21] (the image is always zero-padded to be squared with the side of power of 2),  $r$  and  $\theta$  are the polar spatial frequency coordinates,  $L_0$  and  $H_l$  are low and high pass residuals respectively,  $l$  is the level of the pyramid, and  $A_i$  are band-limited images in the frequency domain. Since the high-frequency image contains little information, it is safely discarded. The band-limited images are created by filtering  $F(r, \theta)$  by multiplying a bandpass filter  $G_i(r)$ :

$$A_i(r, \theta) = F(r, \theta)G_i(r). \quad (2)$$

A popular choice of  $G_i$  is Gaussian filters with various standard deviations. Gaussian filters are closely related to scale space [11] and are widely used in imaging and computer vision. The advantage is that they can be conveniently transformed between the spatial domain and frequency domain. However, the Gaussian filters are asymmetrical in the logarithmic frequency domain, and reconstruction of the input image is nontrivial as filters do not sum to one [21].

Instead, we adapt the cosine-log filter bank [21] for image pyramid generation. A cosine-log filter of 1-octave width, i.e., the central spatial frequency is twice the frequency of the lower cutoff frequency and half of the higher cutoff frequency, centered at frequency  $2^i$  cycles/image is defined as:

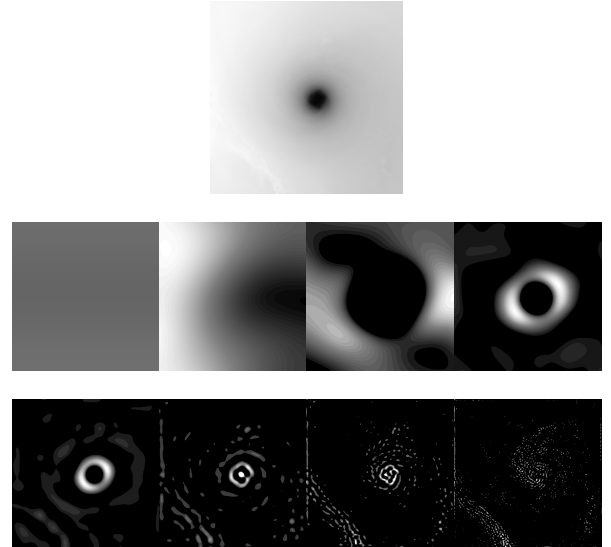
$$G_i(r) = 0.5[1 + \cos(\pi \log_2 r - \pi i)]. \quad (3)$$

Figure 3 shows a 1D example of a cosine-log filter bank comprised of 1-octave-wide cosine-log filters. The shapes are symmetrical in the log spatial frequency axis and the summation of filter responses equals to 1 as shown by the red dash curve. In practice, these filters are defined in the discrete frequency domain and the first few levels occupy only a few pixels. The cosine functions are not accurately represented there. As a result, we slightly change the filter weights at these pixels to make sure that the summation of all filters equal to one, as can be seen in Figure 3.

Bandpass images in the spatial domain  $a_i(x, y)$  are obtained by applying inverse Fourier transform to  $A_i(u, v)$ . Figure 4 shows an image pyramid of 8 levels of the Hurricane Isabel data [6]. It can be seen that the cosine-log filters capture features of different spatial frequencies in the image.

### 3.2 Band Contrast Computation

The average contrast of each bandpass image  $a_i(x, y)$  is calculated and later tested against threshold contrast given by the CSF, which is discussed in the next section. We follow the approach of [21] to obtain contrast images  $c_i(x, y)$  of each



**Figure 4.** Cosine-log image pyramid of the Hurricane Isabel dataset. The input image is shown on the top row; images in the pyramid are shown with increasing spatial frequency from left to right, top to bottom (second and third rows). The bandpass images are amplified for visualization purposes.

pyramid level:

$$c_i(x, y) = \frac{a_i(x, y)}{l_i(x, y)},$$

$$l_i(x, y) = l_0(x, y) + \sum_{j=1}^{i-1} a_j(x, y), \quad (4)$$

where  $l_0(x, y)$  is the low pass residual image in the spatial domain ( $L_0(r, \theta)$  in the polar coordinates frequency domain), and  $l_i(x, y)$  is the low pass image before the  $i$ -th level.

Unlike [21], where the per-pixel representation  $c_i(x, y)$  is used as contrast, we compute an average contrast  $\bar{c}_i$  for level  $i$ . We argue that, in visualization, using per-pixel contrast for the subsequent band weight assignment is problematic for two reasons: first, different amplitudes for pixels in the same band could be confusing and break the mental picture of the user; second, intuitive global luminance transformation for all pixels in a band through user interaction is not possible. Therefore, we calculate the average band contrast  $\bar{c}_i$  for band  $i$ :

$$\bar{c}_i = \frac{\sum_{c_i(x, y) \neq 0} |c_i(x, y)|}{\sum_{c_i(x, y) \neq 0} 1}. \quad (5)$$

Note that other contrast definitions can also be used in our framework.

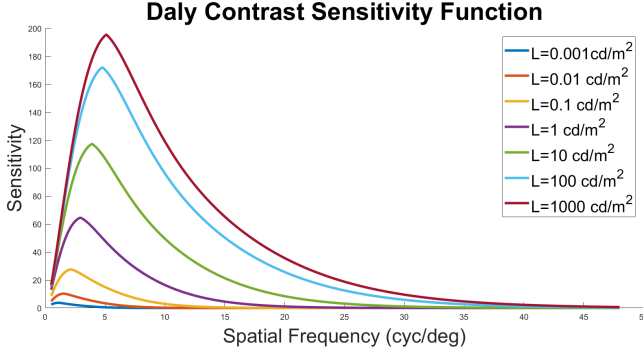


Figure 5. Daly CSFs [4] with various illumination levels.

### 3.3 CSF and Threshold Contrast

The Daly CSF [4] is a comprehensive computational CSF model including many parameters:  $S(r, \theta, L, i^2, d, e)$ , where  $r$  is the radial spatial frequency in cycle/degree (cpd),  $\theta$  is the orientation,  $L$  is the illumination level,  $i^2$  is the image size in degrees,  $d$  is the distance for lens accommodation, and  $e$  is eccentricity. We observe secondary effects on sensitivity for parameters  $\theta$ ,  $d$ , and  $e$ , and it is sufficient for our method to set constant values to these parameters. Figure 5 shows Daly CSFs with various illumination levels  $L$ ; there, the shape of CSFs varies significantly for different  $L$ : higher illumination levels offer better contrast sensitivity; CSF changes from lowpass to bandpass with increasing illumination level. We choose  $L = 100 \text{ cd m}^{-2}$ , which is a typical light condition in an office setting, which is our target environment. As explained in the previous section, we use averaged band contrast, and therefore,  $L$  and  $i^2$  are fixed for a given input image.

Given the CSF, the threshold contrast  $c_t(r)$ , which is used in the viewing distance-based band weight assignment, is simply the inverse of sensitivity  $S$ :

$$c_t(r) = \frac{1}{S(r, 0, 100, i^2, 0.7, 0)} . \quad (6)$$

### 3.4 Virtual Viewing Distance-Based Weight Assignment

The perceptual spatial frequency  $r_p(i)$  in cycles/degree of bands are changed in our method through a virtual viewing distance parameter  $d_v$ . Cosine-log filter bank gives spatial frequency  $r_c(i)$  of each band in cycles/image, and can be converted into the perceptual spatial frequency using Equation 7.

$$\begin{aligned} r_p(i) &= r_c(i) \cdot s_{deg}(I) , i = 0, 1, \dots, l - 1 , \\ s_{deg}(I) &= 2 \cdot \frac{180}{\pi} \arctan \left( 0.5 \frac{s_{cm}(I)}{d_v} \right) , \end{aligned} \quad (7)$$

where  $l$  is the number of layers of the image pyramid,  $s_{deg}(I)$  and  $s_{cm}(I)$  are angle size in degree and physical size in cm of the image  $I$  respectively. The physical size  $s_{cm}(I)$  can be

calculated given the pixel resolution of the image, the pixel resolution, and physical size of the monitor.

Figure 6 shows average band contrast of an image with different viewing distances overlay with a threshold contrast curve  $c_t(r)$  generated by the Daly CSF. It can be seen that with increasing virtual viewing distance, the spatial frequency of bands is increased. Therefore, our method allows for convenient spatial frequency modification of band-limited images with a single virtual viewing distance parameter.

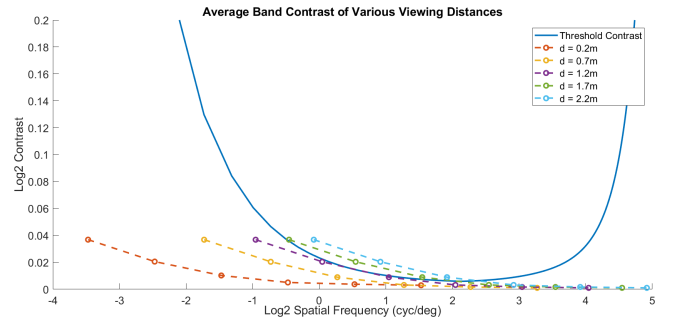
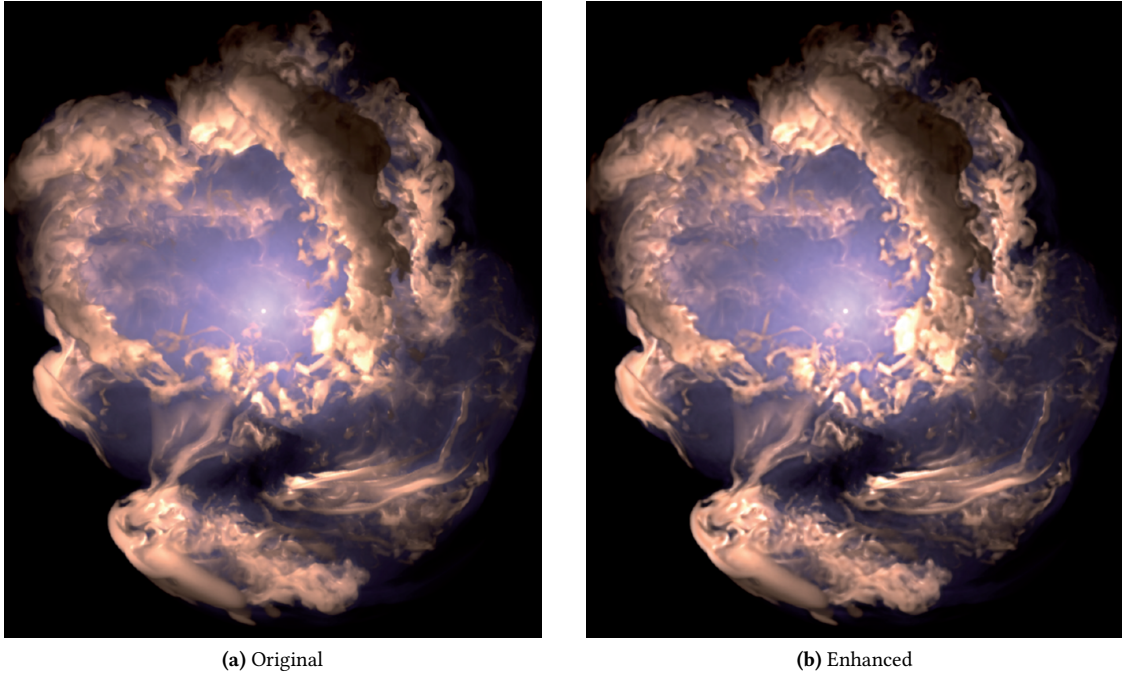


Figure 6. Average contrast of various viewing distance with threshold contrast.

The threshold contrast curve predicts the visibility of features of specific spatial frequency: a feature is not visible if its contrast is below the curve, and it is visible if its contrast sits on or above the curve. Band weight assignment is realized by comparing the average band contrast at virtual perceptual spatial frequencies against the threshold contrast curve. The weight of a band is set to 0, if the band contrast is above the curve; otherwise, the weight is set to be the multiplier that “lifts” the band contrast up to the threshold contrast:

$$w_i = \begin{cases} c_t(r_p(i))/\bar{c}_i - 1 , & c_t(r_p(i)) > \bar{c}_i \\ 0 , & c_t(r) \leq \bar{c}_i \text{ and } r = r_p(i) . \end{cases} \quad (8)$$

It can be seen in Figure 6 that with a short viewing distance, more bands of low spatial frequencies need to be compensated and higher weights are required for shorter viewing distance, e.g.,  $d_v = 0.2\text{m}$ ; with a long viewing distance ( $d_v = 2.2\text{m}$ ); bands with medium spatial frequency typically do not require compensation as threshold contrast is very low for these frequencies, i.e., the contrast sensitivity is very high. These findings successfully match our own experiences in daily life.



**Figure 7.** Volume rendering [1] of a supernova simulation dataset.

### 3.5 Combining Image Channels

The luminance difference image  $f_L(x, y)$  is generated as the weighted sum of band limited images:

$$f_L(x, y) = \sum_1^{l-1} w_i \cdot a_i(x, y). \quad (9)$$

The final visualization  $f_V(x, y)$  is created by combining  $f_L(x, y)$  with the colored image  $f_C(x, y)$ . We replace the achromatic channel  $L(f_C(x, y))$  of  $f_C(x, y)$  by  $L(f_C(x, y)) + f_L(x, y)$ , and keep the chromatic channels of  $f_C(x, y)$  intact.

Care must be taken when band weights are high as the modified achromatic image become saturated, i.e., fully white or black. Since we would like to preserve the appearance of  $f_C(x, y)$  as much as possible, we clamp the achromatic channel  $L(f_V(x, y))$  empirically by  $\pm 20\%$  of the luminance of  $f_C(x, y)$  to give optimal look of the visualization:

$$L(f_V(x, y)) = \min(\max(L(f_V(x, y)), 0.8L(f_C(x, y))), 1.2L(f_C(x, y))).$$

In our current implementation, the combination operation happens in the HSL color space, and the combined color is transformed to the sRGB color space for display.

## 4 User Interaction and Implementation

The virtual viewing distance visualization method has only one parameter—the virtual viewing distance  $d_V$ . Therefore, user interaction is simple and intuitive with our method as  $d_V$  can be easily controlled by a single slider.

The method was implemented in our visualization tool written in C++ using Qt and OpenGL. Our tool supports both 2D images and 3D volume datasets. The cosine-log filter bank was computed only once for an image or a slice of a volume dataset when its size was changed. Image pyramid generation was computed using Fourier transform and was aided by an efficient fast Fourier transform implementation in OpenCV. Contrast image generation was also aided by OpenCV. The computation of these steps took up to a few seconds depending on the size of the image. The CSF was computed once and stored in a lookup table, and weight assignment involved only a few lookups and divisions. The resulting band weights were passed to the GPU, and the luminance image was combined with the color image in a GLSL shader to give the final visualization. As a result, interactivity was achieved with our implementation.

## 5 Examples

The usefulness of our perceptual enhancement is demonstrated through various datasets of different types in this section. Examples range from color mapping on 2D images (slices) to show scalar fields of atmosphere simulation, brain MRI imaging, 3D volume rendered image, all the way to 2D geographic information visualization on maps.

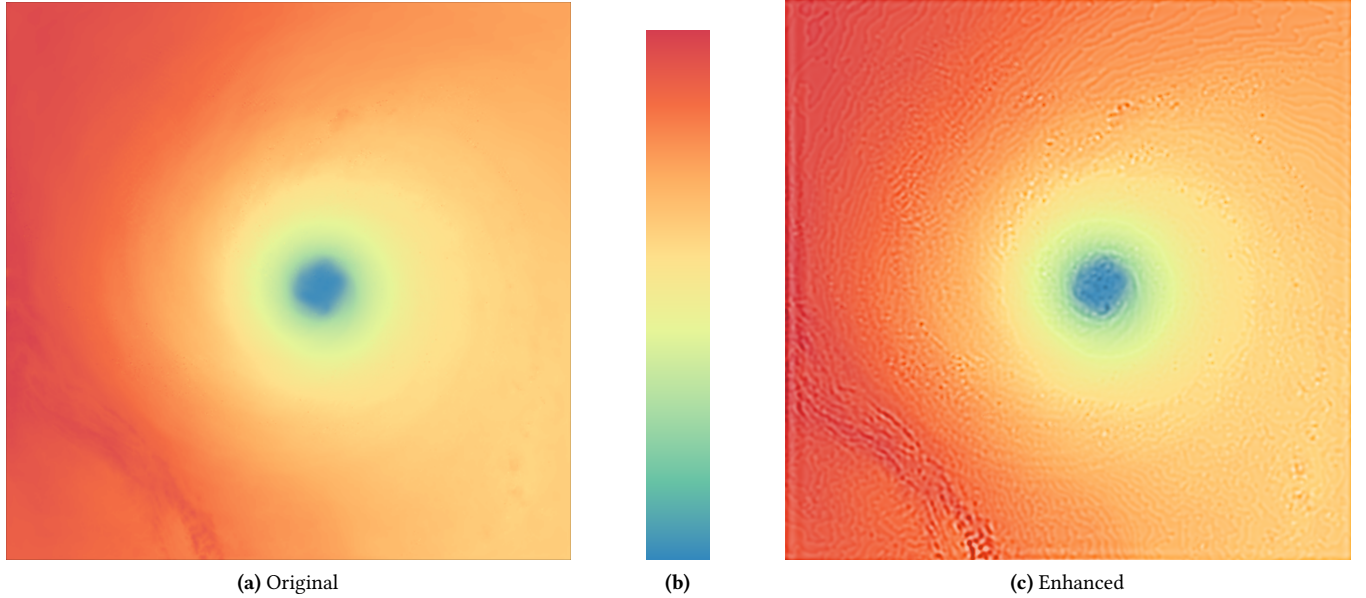


**Figure 8.** Visualizations of the Hurricane Isabel dataset [6]: (a) the original visualization, (b) the color map, and (c) overcompensated with a viewing distance of 200 cm.

## 5.1 Hurricane Isabel

The Hurricane Isabel simulation data shown in Figure 8, is the pressure attribute of time step 29 that well demonstrates the nature of atmosphere simulations which have large-scale smooth, homogeneous structures with subtle yet important vortex details. With a spectrum color map from ColorBrewer<sup>1</sup>, we are able to roughly see the hurricane eye, the spiral arms and the shore area in the input color mapped result. Details outside the hurricane eye can be better seen with a viewing distance of 80 cm with our method (Figure 8(b)). Applying our approach with a viewing distance of 200 cm (Figure 8(c)), the contrast is further enhanced and both the hurricane eye and spiral arm structures are more visible.

## 5.2 MRI brain

Results of an MRI brain scan are shown in Figure 1. The dataset is visualized with a slightly modified isoluminant color map [8]. Without enhancement, the image gives a washed away impression that the brain cannot be easily separated from the surrounding tissues (cyan), and the delicate folded details are not recognizable without difficulty. With a virtual viewing distance of 200 cm, the brain structure with fine details become clearly noticeable, especially for the cerebellum (Figure 1(b)).

### 5.3 Volume Rendered Image

Figure 7 shows volume renderings of a supernova simulation using an ambient scattering model [1]. The perceptual enhanced result (Figure 7(b)) provides a less blurry visualization compared to the original rendering (Figure 7(a)). Specifically, boundaries of complex vortex structures become more prominent with the enhanced contrast, making it easier to gain insights into these structures.

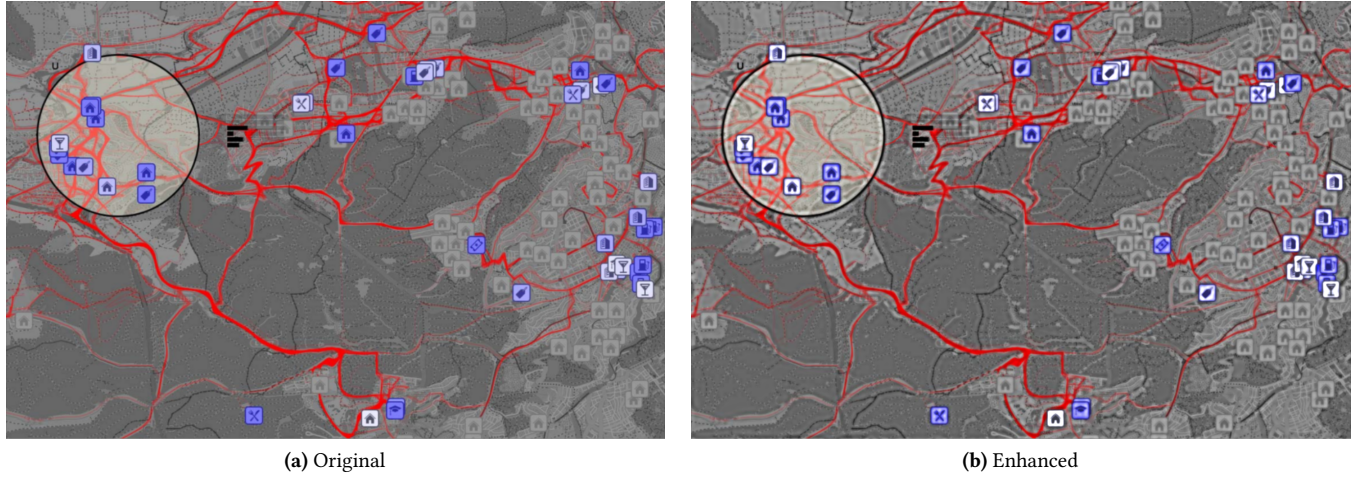
## 5.4 GIS data

Figure 9 shows a visualization of movement behavior [10] on a GIS city dataset. The visualization is designed to achieve a focus-and-context effect: the focus is on dark red road networks and the region inside circle area, other regions are given reduced contrast. The perceptual enhanced result (Figure 9(b)) improves the over-all contrast of the visualization while preserving the focus-and-context feeling. Icons and structures inside the circle of focus become more prominent. Details outside the focus are enhanced so that more insights can be gained easily; nevertheless, the enhancement is not too strong to distract users from the focus region.

## 6 Conclusions

**revise conclusion** In this paper, we have introduced a contrast enhancement method based on virtual viewing distance for data visualization with color images. The perceptually-based enhancement is achieved by adjusting bands that are extracted from the luminance channel of the input image to become visible at a virtual viewing distance. Specifically,

<sup>1</sup><http://colorbrewer2.org>



**Figure 9.** Visualization [10] of a GIS dataset.

the method is built on a multiscale image pyramid created with cosine-log filters; weights of band-limited images are assigned by testing average band contrast against a threshold contrast curve derived from a CSF. Our technique has only a single parameter—virtual viewing distance that can be tuned easily by a slider. Interactivity is achieved with our implementation. The proposed method can be integrated into any visualization pipeline as image post-processing. A wide range of datasets that have representative image features is shown as examples to demonstrate the usefulness of our method. Our viewing distance visualization method is a potential technique that benefits any visualization with effective perceptual enhancement.

## References

- [1] M Ament, F Sadlo, and D Weiskopf. 2013. Ambient Volume Scattering. *IEEE Transactions on Visualization and Computer Graphics* 19, 12 (2013), 2936–2945. <https://doi.org/10.1109/TVCG.2013.129>
- [2] L Bergman, B Rogowitz, and L Treinish. 1995. A rule-based tool for assisting colormap selection. In *Proceedings of IEEE Conference on Visualization '95*. 118–125. <https://doi.org/10.1109/VISUAL.1995.480803>
- [3] F. W Campbell and J Robson. 1968. Application of Fourier analysis to the visibility of gratings. *The Journal of Physiology* 197, 3 (1968), 551–566.
- [4] S. J Daly. 1992. Visible differences predictor: an algorithm for the assessment of image fidelity. , 1666 - 1666 - 14 pages. <https://doi.org/10.1111/12.135952>
- [5] R Fattal, D Lischinski, and M Werman. 2002. Gradient Domain High Dynamic Range Compression. *ACM Transactions on Graphics* 21, 3 (July 2002), 249–256. <https://doi.org/10.1145/566654.566573>
- [6] IEEE. [n. d.]. IEEE Visualization 2004 Contest Data Set. <http://vis.computer.org/vis2004contest/data.html>.
- [7] P Isenberg, P Dragicevic, W Willett, A Bezerianos, and J.-D Fekete. 2013. Hybrid-Image Visualization for Large Viewing Environments. *IEEE Transactions on Visualization and Computer Graphics* 19, 12 (2013), 2346–2355. <https://doi.org/10.1109/TVCG.2013.163>
- [8] G Kindlmann, E Reinhard, and S Creem. 2002. Face-based Luminance Matching for Perceptual Colormap Generation. In *Proceedings of IEEE Conference on Visualization '02*. 299–306. <http://dl.acm.org/citation.cfm?id=602099.602145>
- [9] P Kovesi. [n. d.]. Good Colour Maps: How to Design Them. [arXiv:1509.03700 \[cs.GR\]](https://arxiv.org/abs/1509.03700) 2015.
- [10] R Krueger, D Thom, and T Ertl. 2014. Visual analysis of movement behavior using Web data for context enrichment. In *2014 IEEE Pacific Visualization Symposium (PacificVis)*. 193–200. <https://doi.org/10.1109/PacificVis.2014.57>
- [11] T Lindeberg. 1998. Feature Detection with Automatic Scale Selection. *International Journal of Computer Vision* 30, 2 (01 Nov 1998), 79–116. <https://doi.org/10.1023/A:1008045108935>
- [12] Z Mai, H Mansour, R Mantiuk, P Nasiopoulos, R Ward, and W Heidrich. 2011. Optimizing a Tone Curve for Backward-Compatible High Dynamic Range Image and Video Compression. *IEEE Transactions on Image Processing* 20, 6 (June 2011), 1558–1571. <https://doi.org/10.1109/TIP.2010.2095866>
- [13] R Mantiuk, K J Kim, A G Rempel, and W Heidrich. 2011. HDR-VDP-2: A Calibrated Visual Metric for Visibility and Quality Predictions in All Luminance Conditions. *ACM Trans. Graph.* 30, 4, Article 40 (July 2011), 14 pages. <https://doi.org/10.1145/2010324.1964935>
- [14] S Mittelstädt and D. A Keim. 2015. Efficient Contrast Effect Compensation with Personalized Perception Models. *Computer Graphics Forum* 34, 3 (2015), 211–220. <https://doi.org/10.1111/cgf.12633>
- [15] S Mittelstädt, A Stoffel, and D. A Keim. 2014. Methods for Compensating Contrast Effects in Information Visualization. *Computer Graphics Forum* 33, 3 (2014), 231–240. <https://doi.org/10.1111/cgf.12379>
- [16] K. T Mullen. 1985. The contrast sensitivity of human colour vision to red-green and blue-yellow chromatic gratings. *The Journal of Physiology* 359 (1985), 381–400.
- [17] F. L. V Nes and M. A Bouman. 1967. Spatial Modulation Transfer in the Human Eye. *Journal of the Optical Society of America* 57, 3 (1967), 401–406. <https://doi.org/10.1364/JOSA.57.000401>
- [18] Q Nguyen, P Eades, and S. H Hong. 2013. On the faithfulness of graph visualizations. In *2013 IEEE Pacific Visualization Symposium (PacificVis)*. 209–216. <https://doi.org/10.1109/PacificVis.2013.6596147>
- [19] L Padilla, P. S Quinan, M Meyer, and S. H Creem-Regehr. 2017. Evaluating the Impact of Binning 2D Scalar Fields. *IEEE Transactions on Visualization and Computer Graphics* 23, 1 (Jan 2017), 431–440. <https://doi.org/10.1109/TVCG.2016.2599106>

- [20] S. N Pattanaik, J. A Ferwerda, M. D Fairchild, and D. P Greenberg. 1998. A Multiscale Model of Adaptation and Spatial Vision for Realistic Image Display. In *Proceedings of the 25th Annual Conference on Computer Graphics and Interactive Techniques (SIGGRAPH '98)*. 287–298. <https://doi.org/10.1145/280814.280922>
- [21] E Peli. 1990. Contrast in complex images. *J. Opt. Soc. Am. A* 7, 10 (Oct 1990), 2032–2040. <https://doi.org/10.1364/JOSAA.7.002032>
- [22] E Reinhard, M Stark, P Shirley, and J Ferwerda. 2002. Photographic Tone Reproduction for Digital Images. *ACM Transactions on Graphics* 21, 3 (July 2002), 267–276. <https://doi.org/10.1145/566654.566575>
- [23] B Rogowitz, L. A Treinish, and S Bryson. 1996. How Not to Lie with Visualization. *Computers in Physics* 10, 3 (1996), 268–273. <https://doi.org/10.1063/1.4822401>
- [24] B. E Trumbo. 1981. A Theory for Coloring Bivariate Statistical Maps. *The American Statistician* 35, 4 (1981), pp. 220–226. <http://www.jstor.org/stable/2683294>
- [25] C Ware. 1988. Color sequences for univariate maps: theory, experiments and principles. *IEEE Computer Graphics and Applications* 8, 5 (1988), 41–49. <https://doi.org/10.1109/38.7760>
- [26] A. B Watson and J. A Solomon. 1997. Model of visual contrast gain control and pattern masking. *Journal of the Optical Society of America A* 14, 9 (1997), 2379–2391. <https://doi.org/10.1364/JOSAA.14.002379>
- [27] H. R Wilson. 1991. Psychophysical models of spatial vision and hyper-acuity. *Spatial Vision* 10 (1991), 64–81.
- [28] L Zhou and C Hansen. 2015. A Survey of Colormaps in Visualization. *IEEE Transactions on Visualization and Computer Graphics* PP, 99 (2015), 1–1. <https://doi.org/10.1109/TVCG.2015.2489649>